Available online at www.sciencedirect.com
SCIENCE DIRECT®
Current Opinion in Solid State and Materials Science 8 (2004) 343–352
Current Opinion in Solid State & Materials Science

Nonlinear optical spectroscopy of solid interfaces

Markus B. Raschke [a,*], Y. Ron Shen [b,*]

[a] Max-Born-Institut für Nichtlineare Optik und Kurzzeitspektroskopie, D-12489 Berlin, Germany
[b] Department of Physics, University of California, 94720, Berkeley CA, United States

Abstract

Nonlinear optical spectroscopies for the investigation of solid surfaces and interfaces are reviewed. Emphasis is on the surface-specific second-order nonlinear optical response. Following a brief introduction on the fundamental, a broad variety of applications of second-harmonic (SHG) and sum-frequency (SFG) spectroscopic techniques are discussed. An outlook on exciting new opportunities provided by these techniques is presented.

1. Introduction

Among the various techniques employed for the characterization of surfaces and interfaces, those using light are particularly attractive. They are applicable in situ to all interfaces accessible by light, are nondestructive, and offer unprecedented time-resolution. However, the effective interaction depth of optical radiation in matter is in general at least of the order of a reduced wavelength ($\lambda/2\pi$, as in reflection) which makes isolation of the surface or interface contribution to the optical response from the bulk difficult. The nonlinear optical responses, however, have higher symmetry selectivity compared to linear optics. Since the bulk and surfaces of a material generally have different structural symmetries, they may be selectively probed by nonlinear optics. Specifically, for media with inversion symmetry, the second-order nonlinearity could be dominated by the interface where the inversion symmetry is broken [1–3]. This intrinsic surface-specificity allows for investigations of surface properties not readily accessible by other spectroscopies. The techniques derived from second-harmonic (SHG) and sum-frequency generation (SFG) have thus become powerful and versatile methods for the investigation of surfaces and interfaces [4–6]. Through electronic or vibrational SHG or SFG spectroscopy, information on surface structure, chemical composition and bond or molecular orientation at solid and liquid interfaces can be deduced. This has led to a broad range of surface studies from metals and semiconductors to insulators and magnetic materials, and from liquids to soft condensed matter such as polymers or biological membranes. These investigations are motivated not only by fundamental interests but also for applications such as heterogeneous catalysis, epitaxial growth, electrochemistry, device fabrication, material and environmental problems.

2. Theory

Here, we focus on bulk media with inversion symmetry. Under the electric-dipole approximation, the second-order nonlinear polarization induced in a medium is generally given by

$$P^{(2)}(\omega) = \chi^{(2)}(\omega = \omega_1 + \omega_2)E(\omega_1)E(\omega_2). \quad (1)$$

* Corresponding authors. Tel.: +49 30 6392 1497; fax: +49 30 6392 1489 (M.B. Raschke), tel.: +1 510 642 4856; fax: +1 510 643 8923 (Y.R. Shen).
E-mail addresses: raschke@mbi-berlin.de (M.B. Raschke), shenyr@socrates.berkeley.edu (Y.R. Shen).

1359-0286/$ - see front matter © 2005 Elsevier Ltd. All rights reserved.
doi:10.1016/j.cossms.2005.01.002

Here, $\chi^{(2)}$ denotes the surface nonlinear susceptibility tensor and $E(\omega_1)$ and $E(\omega_2)$ are the pump optical fields with frequencies ω_1 and ω_2, respectively [1,2,7]. From the above equation, it is immediately seen that $P^{(2)}(\omega)$ must vanish in bulk media with inversion symmetry, but becomes nonzero at a surface or interface, where the inversion symmetry is broken [1,2,8,9,11]. Since $P^{(2)}(\omega)$ is the source of the generated output radiation, this makes SHG (with $\omega_1 = \omega_2$) and SFG highly surface-sensitive and specific. However, in some cases, electric-quadrupole and magnetic-dipole contributions to SHG/SFG from the bulk may not be totally negligible. Fortunately, in many cases, it has been shown that the surface contribution to SHG and SFG from a centrosymmetric medium does clearly dominate [12,13].

The sum-frequency output intensity, obtained from the solution of the wave equation with proper boundary conditions, is then given by

$$I(\omega) = \frac{8\pi^3\omega_s^2 \sec^2\theta_\omega}{\hbar c^3\sqrt{\epsilon_1(\omega)\epsilon_1(\omega_1)\epsilon_1(\omega_2)}} \times \left|e^{\dagger}(\omega)\cdot\chi_s^{(2)} : e(\omega_1)e(\omega_2)\right|^2 I_1(\omega_1)I_2(\omega_2). \quad (2)$$

Here $\chi_s^{(2)}$ is the surface nonlinear susceptibility defined by $P_s^{(2)} = \epsilon_0\chi_s^{(2)} : E(\omega_1)E(\omega_2)$, $e(\omega_i) \equiv F(\omega_i)\hat{e}(\omega_i)$, with $F(\omega_i)$ being the transmission Fresnel factor and $\hat{e}(\omega_i)$ the unit polarization vector of $E(\omega_i)$, θ_ω denotes the SF output angle with respect to the surface normal, $\epsilon(\omega_i)$ is the dielectric constant at frequency ω_i, and I_i is the input pump intensity at ω_i.

The surface nonlinear susceptibility $\chi_s^{(2)}$ is a third-rank tensor with 27 tensor elements ($\chi_{ijk}^{(2)}$), many of which vanish or depend on others due to the surface structural symmetry. As an example, $\chi_{ijk}^{(2)}(\omega = \omega_1 + \omega_2)$ for an isotropic surface, with the z-direction defined by the surface normal, has only four independent nonvanishing elements: $\chi_{xxz}^{(2)} = \chi_{yyz}^{(2)}$, $\chi_{xzx}^{(2)} = \chi_{yzy}^{(2)}$, $\chi_{zxx}^{(2)} = \chi_{zyy}^{(2)}$, and $\chi_{zzz}^{(2)}$. Different combinations of input and output beam polarizations in SFG measurements can be used to deduce values for the nonvanishing tensor elements. Such measurements then allow the determination of surface symmetry or/and surface molecular orientation. Being a third-rank tensor, $\chi_s^{(2)}$ can reflect up to three-fold rotational symmetry. The macroscopic quantity $\chi_{s,ijk}^{(2)}$ is related to the molecular nonlinear polarizability or hyperpolarizability $\alpha_{\xi\eta\zeta}^{(2)}$, where $\hat{\xi}$, $\hat{\eta}$, and $\hat{\zeta}$ define the molecular coordinates, through the coordinate transformation

$$\chi_{s,ijk}^{(2)} = N_s\left\langle(\hat{i}\cdot\hat{\zeta})(\hat{j}\cdot\hat{\eta})(\hat{k}\cdot\hat{\xi})\right\rangle\alpha_{\xi\eta\zeta}^{(2)}. \quad (3)$$

The angular brackets here denote an average over the molecular orientational distribution, and N_s is the surface molecular density. For simplicity, the microscopic local-field correction is neglected in Eq. (3). Knowing $\chi_{s,ijk}^{(2)}$ and $\alpha_{\xi\eta\zeta}^{(2)}$ thus permits deduction of information on the molecular orientation.

An explicit expression for the nonlinear optical polarizability is obtained from a second-order quantum mechanical perturbation calculation:

$$\alpha_{s,ijk}^{(2)}(\omega_s) = -\frac{e^3}{\hbar^2}\sum_{g,n,n'}\left[\frac{\langle g|r_i|n\rangle}{\omega_s - \omega_{ng} + i\Gamma_{ng}}\left(\frac{\langle n|r_j|n'\rangle\langle n'|r_k|g\rangle}{\omega_2 - \omega_{n'g} + i\Gamma_{n'g}} + \frac{\langle n|r_k|n'\rangle\langle n'|r_j|g\rangle}{\omega_1 - \omega_{n'g} + i\Gamma_{n'g}}\right) + \cdots\right]\rho_g^{(0)}. \quad (4)$$

This expression, containing a total of 8 terms, shows how the nonlinear polarizability or susceptibility depends on material parameters such as the dipole transition moments $\langle n|r_i|g\rangle$ and energy levels. The quantities ω_{ng} and Γ_{ng} are the frequencies and half widths for the transitions between quantum states $|n\rangle$ and $|g\rangle$, and $\rho_g^{(0)}$ denotes the population in $|g\rangle$. It can be seen that $\alpha^{(2)}$, and hence the SF output, are resonantly enhanced when the pump frequency ω_1 or ω_2 and/or the sum frequency $\omega_1 + \omega_2$ approach resonance. The resonant enhancement provides spectral information on electronic or vibrational transitions, or more generally, any surface characteristic transitions.

3. Experimental

For SHG and SFG experiments, in general, pulsed pump radiation is directed onto the surface as shown schematically in Fig. 1. Tunable laser pulses can be obtained from optical parametric generation and amplification (OPG/OPA), together with harmonic, sum- or difference-frequency generation, pumped by ps or fs lasers. Tuning range can be extended from near UV at ~200 nm to mid IR at ~18 μm (see [14–16] and references therein). For SFG, the two input pulses at ω_1 and ω_2 are directed to overlap spatially and temporally on the sample. In detection, the signal must be discriminated against reflected and scattered pump light. This is achieved by spatial and spectral filtering with apertures

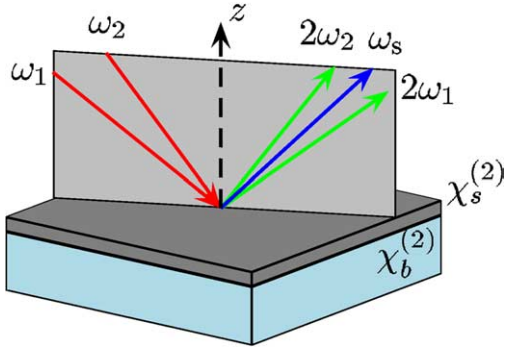

Fig. 1. Schematic of SHG/SFG geometry in reflection from a surface or interface. Pulsed pump radiation overlaps spatially and temporally on the surface and the generated second-harmonic ($2\omega_1$ and $2\omega_2$) or sum-frequency ($\omega_s = \omega_1 + \omega_2$) radiation in reflection is detected.

and spectral filters. A monochromator is sometimes needed for additional stray-light suppression. The signal is detected by a photomultiplier and gated electronics or a CCD array.

From Eq. (2) the expected signal strength for SHG/SFG can be estimated. With a typical value of $\chi_s^{(2)}$ of 10^{-21} m^2 V^{-1}, a pump pulse of 1 μm in wavelength, incident at $\theta = 45°$ and having pulse energy $E = IA\tau =$ 100 μJ, beam cross-section $A = 1$ mm^2, and pulse duration $\tau = 10$ ps, can generate about 10^3 SH photons. With a photon counting detection system, a minimal count rate of 10^{-3} photons/pulse can be achieved that would allow detection of $\chi_s^{(2)}$ as small as 10^{-24} m^2 V^{-1}. In practice, the limit is often set by the time one can devote to the measurement. In order to obtain accurate spectra or absolute values for $\chi_{s,ijk}^{(2)}$ of the material investigated, the results must be normalized against those of a reference material with known dispersion and known values of $\chi^{(2)}$, such as z-cut quartz.

The simplest kind of experiments are SHG at a fixed pump frequency. From its response to surface modification, one can probe kinetics and dynamics of adsorption, desorption, diffusion, melting and phase transitions of a surface. Tuning the pump wavelength gives, in addition, information about surface electronic transitions. For surface vibrational spectroscopy, however, SHG output is in the infrared where the photodetector is much less sensitive, and IR–vis SFG is more advantageous. In the latter case, tunable IR input is mixed with visible input to yield a SF signal in the visible region that can be more readily detected.

4. Surface specificity

A note on the definition of surface or interface is in order. In SHG and SFG, the surface or interface layer refers to a thin sheet between two adjacent bulk media that has a different structure from the bulk. For bulk media with inversion symmetry, if the surface layer is polar-ordered, then its contribution to SHG and SFG often dominates over the bulk reponse. The bulk contribution from electric-quadrupole and magnetic-dipole terms may not be negligible, and separation of surface and bulk contributions in SHG and SFG is a subtle problem in general [3,8,9]. Experimentally, however, the effect of surface modification on SHG/SFG can be used to test the importance of bulk contribution and separate surface and bulk contributions. More generally, because surface and bulk symmetries of a medium are usually different, polarization selection rules for different symmetries can sometimes be used to separate the two contributions. This is the case even for a medium without inversion symmetry, for example, III–V and II–VI semiconductors such as GaAs and ZnSe, where SHG/SFG is electric-dipole allowed and very strong in the bulk [17]. With an appropriate choice of polarization combinations and surface orientation, the bulk contribution can nevertheless be well suppressed, allowing for the distinct observation of the surface or interfacial SFG or SHG from these systems.

5. Applications

Both SFG and SHG have been applied to a wide variety of surface and interfacial systems. They have made possible the investigation of surfaces and interfaces under ambient, high pressure, and nearly arbitrary temperature conditions. Moreover, they have provided access to buried interfaces between solids or liquids. Progress in the field has been discussed in a number of review articles [3–6,16,18–35]. Here, we focus on some unique applications of the techniques to illustrate the capabilities and versatility of SHG and SFG as surface spectroscopic tools for solids.

SHG and SFG were first developed to study molecular adsorbates on solid surfaces [36–41]. In particular, it was shown that SHG could be used to probe adsorption and desorption of atoms and molecules on metals and semiconductors in ultrahigh vacuum (UHV) [40]. The adsorbate alters the electronic properties of the interface and a corresponding variation of the SHG signal can be related to the surface density of the adsorbate. The technique can also be extended to studies of surface association and dissociation of molecules. There already exist quite a few review articles on this subject [3,6,18–20,22,23,32]. The capability of SHG for in situ probing during gas exposure together with its sub-monolayer sensitivity even allows for investigation of competing reaction channels on a surface [42].

One can also use SHG to probe lateral surface reactions, e.g., surface diffusions [43]. One example is the study of thermally induced hydrogen diffusion between steps and terraces on Si(0 0 1) [42,44]. Because of the reduced symmetry of stepped surfaces, SHG can be selectively sensitive to step or terrace sites, respectively, and therefore used to monitor adsorbates at step and terrace sites. As shown in Fig. 2 the thermally activated diffusion process associated with depletion of the hydrogen population at the steps can be followed by SHG. The result then permits deduction of the diffusion activation energy—a key parameter for the understanding of important surface processes involving hydrogen as reactant or reaction intermediate.

The intrinsic surface specificity of SHG/SFG permits studies of molecular adsorption on substrates even under high-pressure gas atmosphere and at liquid–solid interfaces. This makes the techniques truly distinct from most other surface probes that are limited to the UHV environment. Thus they provide opportunities for research in several neglected areas of surface science. As

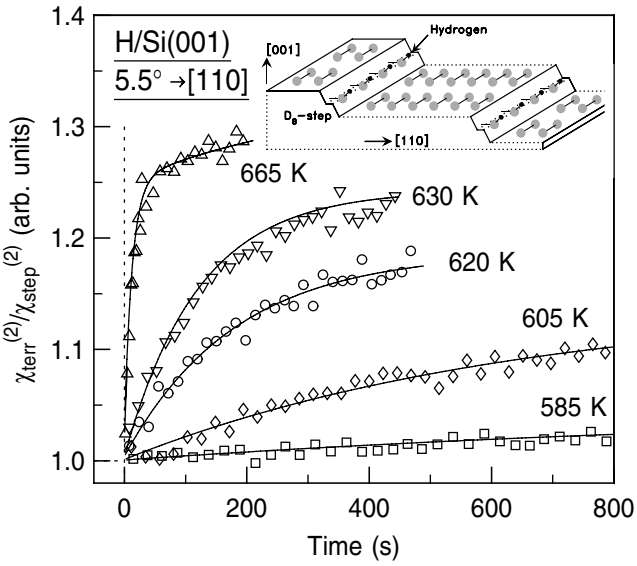

Fig. 2. Sensitivity of SHG with respect to different adsorption sites allows probing of the kinetics of hydrogen diffusion from initially hydrogen saturated step sites onto terraces of Si(0 0 1) 5.5° → [1 1 0]. From the temperature dependence an Arrhenius activation energy of 1.7 eV is derived. The continuing signal increase observed at $T = 665$ K is due to the onset of recombinative hydrogen desorption (after [44]).

an example, SHG can be employed to probe adsorbates on a surface in true thermal equilibrium with gas atmosphere at any realistic temperature. Being capable of deducing surface coverage of adsorbates, it allows for direct isosteric heat measurements. This has successfully been applied to the determination of the chemisorption energy of H_2 on Si(1 1 1)7×7 and Si(0 0 1)2×1 [45].

Sum-frequency vibrational spectroscopy (SFVS) is more selective in identifying adsorbate species through their vibrational modes and often also more sensitive because of the vibrational resonance enhancement. It can be used for selective probing of adsorbed species and competitive adsorption of species. The adsorption sites and bond orientations of adsorbates can also be determined. Adsorption of water on metal surfaces [46,47] is an example. The formation of a hydrogen-bonding network that approaches an ice-like structure with increasing coverage has been observed. Among investigations of adsorption under ambient conditions, the SFG study of water adsorption on mica, in equilibrium with water vapor in atmosphere with different humidities, is representative. In this experiment, evolution of the interfacial water structure with increasing humidity from an initially disordered structure at submonolayer coverage into an ordered hydrogen-bonded network at full monolayer coverage has been observed for the first time [48].

Since the early days of surface science, the question of how the adsorbed species and their geometries that appear on a substrate under high vapor pressure compare with those under UHV has been outstanding. This question is now possible to be addressed by SFVS [49,50]. New adsorbate arrangement and more weakly bound adsorbate species, for example, showed up with higher surface density on Pt(1 1 1) or Pd nanoparticles under high-pressure CO gas [30,51,52].

Practically useful heterogeneous catalysis generally occurs under real atmosphere, but research is often conducted in UHV environment. The use of SFVS as a probe is able to bridge this pressure gap [30,53,54]. The important case of CO oxidation on Pt, first studied by Langmuir, is a good example. In UHV, CO adsorbes mainly at the top and bridge sites of Pt(1 1 1) and therefore one would suspect that these species were responsible for the catalytical reaction of CO oxidation. Under high pressure of CO and O_2, however, it was found that the CO oxidation rate is directly related to the surface density of CO adsorbed at incommensurate sites [55]. Catalytic combustion of CO on both crystalline and rough polycrystalline Pt as well as on supported nanoparticles of Pd has also been investigated [52,55,56]. Other examples are methane dissociation on diamond [57] and ethylene hydrogenation on Pt(1 1 1) and Rh(1 1 1) with the poisoning effect of CO [58–60]. More recently, high-pressure ammonia adsorption and dissociation on clean Fe(1 1 1) as well as oxygen-precovered Fe(1 1 1) have been investigated—a key study which shed light on the intriguing role of iron as catalyst in this important catalytic process [61].

With the help of ultrashort laser pulses, SHG and SFG allow for probing surface processes on ultrafast time scales [62–65]. Hydrogen on silicon and CO on metal served as model systems to demonstrate the capabilities of SFVS to probe surface vibrational dynamics [66]. In IR-pump/SFG-probe experiments, population relaxation (T_1) of vibrational excitation and energy transfer can be accessed. The SF photon echo scheme permits measurement of the dephasing time, T_2, of the vibrational excitation [25,65,67,68]. Time-resolved SFVS also provides the opportunity to take snapshots of reaction intermediates. In a representative experiment, the dynamics of desorption and reaction of CO on Ru(0 0 1) was probed on a picosecond time scale [69,70]. Fig. 3 shows how the spectrum of the C–O stretch vibrations varies after the excitation of Ru(0 0 1) by a 800-nm, 110-fs pump pulse. Transient heating of the surface from an initial temperature of 340 K to 1000 K led to desorption of about 50% of CO. Correspondingly, the C–O stretch frequency exhibits a strong transient redshift. These experiments demonstrate the potential of time-resolved SFVS to probe surface dynamics. The technique could also be used to probe reaction intermediates and product formation in a surface reaction in real time, providing direct access to the underlying microscopic reaction mechanisms.

Both SHG and SFG are not limited to the solid–gas or –vapor interface. They can be used to study, for

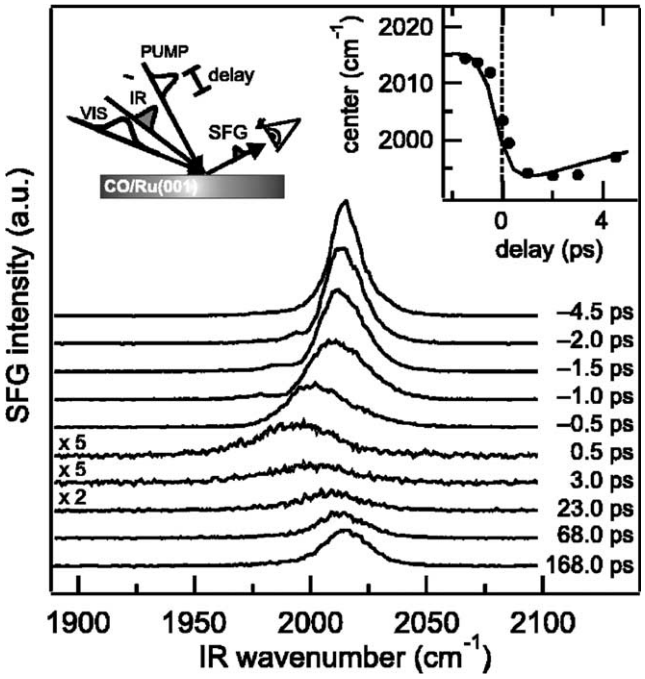

Fig. 3. Transient SFG spectra of the C–O stretch vibration after excitation with a 800 nm/110 fs pump pulse. Starting at a temperature of 340 K and a CO coverage of 0.33 ML the transient heating of the surface up to 1000 K leads to desorption of about 50% of the molecules (after [71]).

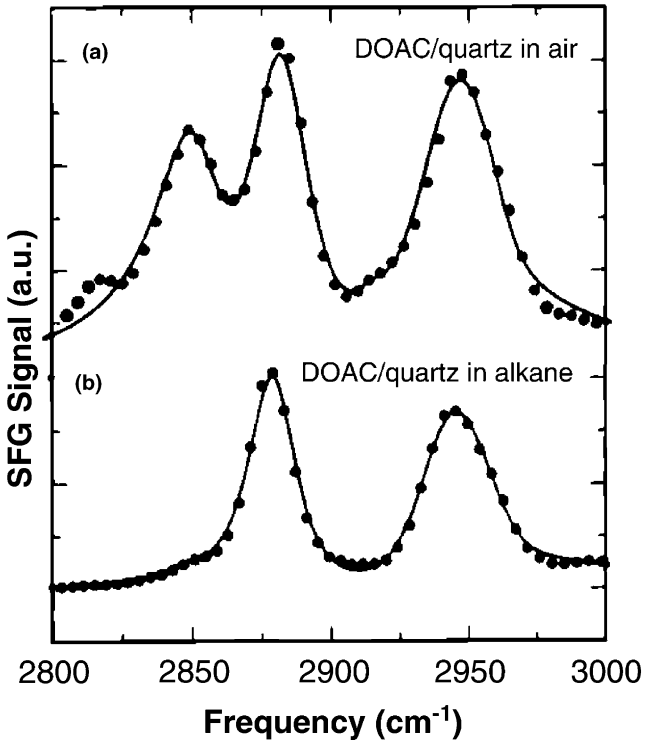

Fig. 4. Sum-frequency vibrational spectra of a DOAC monolayer with a C_{16} chain length on quartz exposed to air (a) and immersed in deuterated alkane (b). The conformational order is reflected by the CH_2 symmetric stretch mode at ~2850 cm^{-1}. It is related to the density of gauche defects in the surfactant alkyl chain (after [48]).

example, electrochemistry at solid–liquid interfaces. In combination with voltammetry, they provide in situ information on oxidation and reduction of adsorbates at the electrochemical interfaces [26,37,72–75]. SFVS, in particular, can identify the adsorbed species and their bond orientation—information virtually inaccessible by other experimental techniques. Recent examples in this area are the observation of significant perturbation of CO bonding to Pt(1 1 1) by the oxidation potential [76,77], and potential-induced reorientation of acetonitrile adsorbed on Pt(1 1 1) [74,78].

SFVS has been widely adopted to study self-assembled surfactant monolayers on insulator, metal and semiconductor surfaces in air or liquids [16,21,31,48,79–84]. It provides a wealth of structural information on the surfactant monolayers, including chain conformation as a function of molecular surface density, molecular chain length, temperature and environment such as the polarity of the adjacent liquid. As an example, Fig. 4 shows the SF vibrational spectra of a dioctadecyldimethylammonium chloride (DOAC) monolayer self-assembled and covalently bound to a quartz surface in air and in deuterated alkane [48]. The two peaks at ~2875 cm^{-1} and ~2940 cm^{-1} are due to the CH_3 symmetric stretch and its Fermi resonance with the bending mode. The presence of the CH_2 symmetric stretch at ~2850 cm^{-1} is an indication that the alkyl chains are not in the all-trans conformation in air (Fig. 4a). In contrast, bringing the sample in contact with long-chain alkane (Fig. 4b) suppresses the CH_2 peak, suggesting that the gauche defects in the DOAC chains have been eliminated. Insertion of the alkane molecules into the surfactant monolayer must have provided enough chain-chain interaction for the surfactant chains to straighten up. This example serves to illustrates the strength of SFVS over linear IR spectroscopy. The IR spectra of the monolayer would be dominated by CH_2 because of their relatively large number present in the chain, but the SF spectra dictated by symmetry, strongly suppress the contribution of CH_2 if the chains are ordered.

The above studies have paved the way to applications of SFVS to investigation of bio-mimetic interfaces and biological functions of complex molecular systems. Both SHG and SFG have been applied to selected systems, ranging from protein adsorption at interfaces [85] to isomerization of retinal molecules [86]. Recently, the phase diagram of self-organizing phosopholipid model membranes, the key constituents of cell membranes, was probed by SFVS [87]. The effect of molecular density and temperature on the spectrum provides information on intermolecular interactions and phase transitions.

SHG and SFG have proven to be particularly valuable for investigation of surfaces of homogeneous bulk

liquids and solids. For example, they have found widespread applications in the instigation of polymer surfaces [88–91]. Because of the sensitivity of different parts of polymer units to the surrounding, a polymer surface may have very different composition and structure than the bulk. SFVS is a powerful tool to probe polymer surfaces at the molecular level. Its use to investigate whether the glass transition of the polymer surface is different from that of the bulk is an example [92]. In many applications, one would like to have a polymer surface design-made while keeping the bulk property unchanged. This can be achieved by, e.g., doping the polymer or modifying terminals of polymer units. SFVS is a helping tool for such design work [91,93]. The surface structure of a polymer could also respond to changes of the environment; for example, the hydrophilic or hydrophobic parts of the polymer units at the surface would emerge depending on whether the surface is exposed to water or air, as revealed by SFVS [91,94,95].

External perturbation can also modify a polymer surface. Mechanical rubbing, for example, can effectively align the surface polymer chains along the rubbing direction. Using SFVS with different input/output polarization combinations with respect to the sample geometry, one can deduce from the measurement quantitative information on how the surface chains are aligned and their constitutive molecular groups are oriented on the rubbed surface [89]. The rubbed polymer surface is commonly used in the industry to align liquid crystal films for display devices. To understand how this happens, SHG has been effectively used to probe alignment of the first liquid crystal monolayer at the polymer surface and the subsequent alignment of the liquid film through molecular correlation [96,97]. Structural changes of polymer surfaces upon mechanical pressure have also been observed [98]. They reveal complex behavior due to the interplay of viscoelastic properties and surface free energy. SHG and SFVS can be extended to studies of amphiphilic macromolecules at solid/liquid interfaces [95]. Adsorption, desorption, and conformational changes of polypeptides and proteins on substrates of different surface hydrophobicity as well as different physiological conditions (pH, ionic concentration) have been studied. They provide insight into the mechanism of denaturation of proteins and reveal pathways for conserving protein function.

SHG/SFG can also be used for in situ probing of surfaces of bulk crystals. Study of surface melting of ice in equilibrium with its vapor is an example [99]. This allowed to directly probe the surface disorder transition and surface melting. As depicted in Fig. 5, the spectrum of the (0001)-ice/vapor interface in the OH stretch region exhibits a strong temperature dependence. In particular, the narrow peak at ($\sim$3700 cm^{-1}) from the dangling OH bonds at the surface decreases in strength

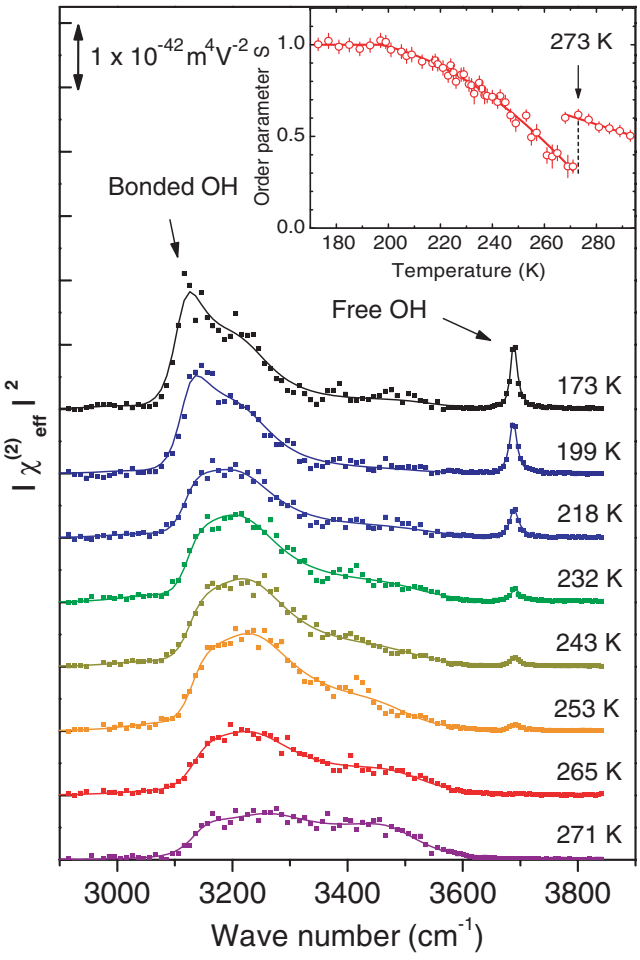

Fig. 5. Sum-frequency vibrational spectra in the OH-stretch region of the vapor/ice interface (ppp polarization combination). The narrow peak at 3700 cm^{-1} comes from the stretch vibration of the dangling OH bonds at the surface. The broad resonance at lower wave numbers originates from hydrogen-bonded OH groups. Inset: The temperature dependence of the orientational order parameter for the dangling OH-bond serves as a measure of the surface disorder and shows when surface melting starts to occur (after [99]).

with increase of temperature after 200 K and becomes not detectable after $\sim$255 K, indicating that the onset of surface melting of ice is as low as $\sim$200 K.

In earlier experiments, SHG was used to probe crystalline silicon surfaces. Different surface symmetries associated with different surface phases allow SHG to monitor surface structural transitions, e.g., Si(1 1 1)$(2\times1)\rightarrow(7\times7)$ [100] and Si(1 1 1)$(7\times7)\rightarrow(1\times1)$ [101]. It was also used in pump/probe measurements to probe laser-induced melting of surface layers of metals and semiconductors [102–104].

With tunable lasers, SHG can also probe surface electronic states of metals and semiconductor surfaces and interfaces (see [33,105–107] and references therein). For example, from the surface SHG spectrum, surface electronic states of Si can be identified and characterized [33,108,109].

Unique for SHG and SFG is also its capability to interrogate solid/solid interfaces. An early example concerns the CaF_2/Si(1 1 1) interface where the hybridized interface electronic states of occupied and unoccupied Si(3p)–Ca(4s) were identified by SHG [110]. Similar studies on Si/SiO_2 [111,112], and ZnSe/GaAs(0 0 1) interfaces [113] were reported. In the latter case, although both ZnSe and GaAs bulks are SHG-active for lack of inversion symmetry, it is still possible to make SHG interface-specific. This is because the different symmetries between bulk and interface allows suppression of bulk contribution to SHG by using specific input/output polarization combination. Interfacial transition between the valence state of ZnSe and the quantum well state of GaAs was detected (with similar investigation addressing the metal/GaAs interface) [114].

The second-order magneto-optical response with selective input/output polarization combinations can also be surface- and interface-specific [115,116]. Magnetization-induced SHG has been used to probe surface and interface magnetizations of ultrathin ferromagnetic films, bimetallic systems and multilayers and superlattices [106,117–121]. Such nonlinear magneto-optical Kerr effect has also been employed in magnetic imaging for visualization of magnetic domains and domain walls [122]. SHG probing of the magnetization dynamics following electronic excitations of magnetic metals or alloys by ultra-short laser pulses can yield information about coupling of spins with electronic degrees of freedom as SHG can distinguish spins from the electronic subsystem [123].

6. Outlook

Although, as described in the previous section, SHG and SFG have already become established analytical tools for surface investigations with widespread applications in diverse areas, improvement of the techniques allows still more novel and specific applications. For example, ongoing progress in laser technology and signal detection provides ever increasing sensitivity that has enabled SFG/SHG microscopy [124–126] and surface studies on the nanoscale [87,127–132].

It has only recently been demonstrated that doubly-resonant infrared-visible SFG, as a two-dimensional spectroscopy, can be highly selective to probe coupling between surface vibrational and electronic transitions [133,134]. With both ω_{IR} and ω_{vis} tuned over surface vibrational and electronic resonance, respectively, SFG is doubly resonantly enhanced if vibronic coupling exists. In much the same way as resonant Raman spectroscopy for studies of intra- and inter-molecular vibronic coupling, doubly-resonant SFG provides similar opportunities for investigation of molecules at interfaces. An example is shown in Fig. 6 describing the enhancement

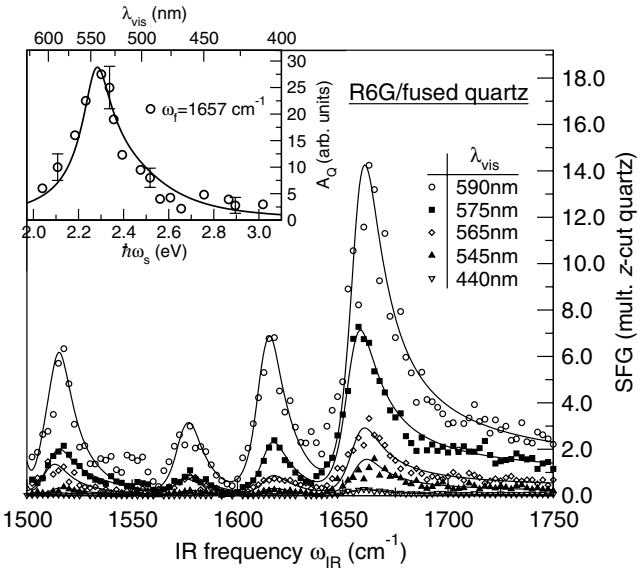

Fig. 6. Doubly-resonant sum-frequency vibrational spectra of a molecular monolayer of Rhodamine 6G molecules adsorbed on fused quartz in the ssp polarization combination. The spectra are resonantly enhanced as $\omega_s = \omega_{vis} + \omega_{IR}$ approaches the molecular S_0–S_1 electronic transition. Inset: Excitation spectrum of the double resonant SFG for the 1657 cm^{-1} mode (after Ref. [134]).

of the SF vibrational spectrum of a monolayer of rhodamine 6G adsorbed on fused silica when $\omega_s = \omega_{vis} + \omega_{IR}$ is tuned over the S_0–S_1 resonance [134]. From the result, the relative vibronic coupling strength between different vibrational modes and the S_0–S_1 electronic transition could be deduced. The double resonance also led to an unprecedented surface sensitivity of SFVS. Recently, the technique has been applied to detect the elusive charge transfer state of CO on Pt(1 1 1) [135].

In most SHG and SFG measurements, only the signal intensity is measured, and hence only the magnitude of the corresponding nonlinear susceptibility element, $\chi_s^{(2)}$, is deduced. Knowledge of the phase of $\chi_s^{(2)}$ is nevertheless important as it can provide, for example, information on absolute bond or molecular orientation [136–138]. Yet to date, few studies have explored this potential of SHG and SFG spectroscopy.

So far, SHG and SFG have been primarily employed for investigation of planar surfaces, but recently, their applications to surfaces of nanostructures have been demonstrated [127–130,139,140]. Unlike the case of planar surfaces, the output from nanostructures is not directional, but resembles that of Mie scattering [127,129,140]. The selection rules are also different [10,128,130]. One distinctive feature is that bulk contributions from higher-order multipoles of the polarization can be separated from the local interfacial contributions in some cases. This enables separation of local surface and nonlocal bulk contributions and allows for simultaneous surface and bulk investigations for partially

asymmetric nanostructures [130]. This may provide new opportunities for investigation of surface structure and molecular adsorption on nanoparticles or nanostructured surfaces.

Currently, the spectral range of SFVS is limited to $\lambda_{IR} < 16\ \mu m$ by the availability of tunable coherent source in the infrared. It prevents us from studying low-frequency vibrational modes of molecular adsorbates, surface phonons of most solids, and other low-frequency surface excitations. Tera-Hertz generation by femtosecond laser pulses, however, may change the situation in the near future. Probing of deep UV electronic resonances of surfaces and interfaces is another problem neglected due to lack of suitable coherent sources.

Many areas of solid surface science are yet to be further explored by SHG and SFG. For example, important electrochemical reactions such as photo-dissociation of water molecules and metal corrosion have not yet been studied. The remote sensing ability of the techniques to probe surfaces in hostile environment has hardly been utilized. Important surface problems like tribology, plasma deposition or treatment of surfaces, and environmental surface reactions have not yet been carefully investigated. The study of burried interfaces have also been limited to a few selected model systems. In situ monitoring of surface modification is important for many applications, and SHG/SFG are yet to be adopted as analytical tools for such purpose.

In summary, we have illustrated the potential of SHG and SFG as unique powerful surface probes for a vast variety of interfacial systems hardly accessible by most other spectroscopies. The techniques are already well established in many areas of surface science, but expansion into broader areas are anticipated upon further exploration.

Acknowledgment

This work was supported by the Director, Office of Energy Research, Office of Basic Energy Sciences, Materials Science Division of the US Department of Energy under Contract No. DE-AC03-76SF00098.

References

[1] Shen YR. The principles of nonlinear optics. New York: Wiley; 1984.
[2] Bloembergen N. Nonlinear optics. New York: Benjamin; 1977.
[3] Heinz TF. In: Ponath H-E, Stegeman GI, editors. Nonlinear surface electromagnetic phenomena. Amsterdam: North-Holland; 1991. p. 353.
[4] Shen YR. Frontiers in laser spectroscopy. In: Hänsch TW, Inguscio M, editors. Proc Int School of Physics Enrico Fermi, Course CXX. Amsterdam: North-Holland; 1994. p. 139.
[5] Huang JY, Shen YR. In: Ho W, Dai HL, editors. Laser spectroscopy and photochemistry of metal surfaces. Singapore: World Scientific; 1995. p. 5.
[6] Matthias E, Träger F, editors. Special issue: nonlinear optics at interfaces. Appl Phys B 1999;210.
[7] Boyd RW. Nonlinear optics. San Diego: Academic Press; 1992.
[8] Koopmans B, van der Woude F, Sawatzky GA. Phys Rev B 1992;46:12780.
[9] Sipe JE, Mizrahi V, Stegeman GI. Phys Rev B 1987;35:9091.
[10] Roke S, Bonn M, Petukhov AV. Phys Rev B 2004;70:115106.
[11] Petukhov AV, Brundy VL, Mochán WL, Maytorena JA, Mendoza BS. Phys Rev Lett 1998;81:566.
[12] Guyot-Sionnest P, Shen YR. Phys Rev B 1988;38:7985.
[13] Held H, Lvovsky AI, Wei X, Shen YR. Phys Rev B 2002;66:205110.
[14] Elsaesser T, Seilmeier A, Kaiser W, Koidl P, Brandt G. Appl Phys Lett 1984;44:383.
[15] Kaindl RA, Wurm M, Reimann K, Hamm P, Weiner AM, Wörner M. J Opt Soc Am B 2000;17:2086.
[16] Buck M, Himmelhaus M. J Vac Sci Technol A 2001;19:2717.
[17] Stehlin T, Feller M, Guyot-Sionnest P, Shen YR. Opt Lett 1988;13:389.
[18] Shen YR. Annu Rev Phys Chem 1989;40:327.
[19] Eisenthal KB. Annu Rev Phys Chem 1992;43:627.
[20] Shen YR. Int J Nonlinear Opt Phys 1994;3:459.
[21] Bain CD. J Chem Soc Faraday Trans 1995;91:1281.
[22] Eisenthal KB. Chem Rev 1996;96:1343.
[23] Reider GA, Heinz TF. In: Halevi P, editor. Photonic probes of interfaces. Amsterdam: Elsevier; 1995. p. 413.
[24] McGilp JF. Prog Surf Sci 1995;49:1.
[25] Guyot-Sionnest P, Harris AL. In: Ho W, Dai HL, editors. Laser spectroscopy and photochemistry of metal surfaces. Singapore: World Scientific; 1995. p. 405.
[26] Tadjeddine A, Peremans A. Surf Sci 1996;368:377.
[27] Shen YR. Solid State Commun 1997;102:221.
[28] Gragson DE, Richmond GL. J Phys Chem 1998;102:3847.
[29] Schultz MJ, Schnitzer C, Simonelli D, Baldelli S. Int Rev Phys Chem 1999;19:123.
[30] Somorjai G, Rupprechter G. J Phys Chem B 1999;103:1623.
[31] Miranda PB, Shen YR. J Phys Chem B 1999;103:3292.
[32] Dumas P, Weldon MK, Chabal YJ, Williams GP. Surf Rev Lett 1999;6:225.
[33] Downer MC, Mendoza BS, Gavrilenko VI. Surf Interf Anal 2001;31:966.
[34] Shen YR. In: Morra M, editor. Water in biomaterials surface science. Chichester: Wiley; 2001. p. 215.
[35] Raschke MB, Shen YR. In: Guenther B, et al, editors. Encyclopedia of modern optics. London: Academic Press; 2004.
[36] Chen JM, Bower JR, Wang CS, Lee CH. Opt Commun 1973;132:132.
[37] Chen CK, Heinz TF, Ricard D, Shen YR. Phys Rev Lett 1981;46:1010.
[38] Heinz TF, Chen CK, Ricard D, Shen YR. Phys Rev Lett 1982;48:478.
[39] Heinz TF, Tom HWK, Shen YR. Phys Rev A 1983;28:1883.
[40] Tom HWK et al. Phys Rev Lett 1984;52:348.
[41] Zhu XD, Suhr H, Shen YR. Phys Rev B 1987;35:3047.
[42] Kratzer P, Pehlke E, Scheffler M, Raschke MB, Höfer U. Phys Rev Lett 1998;81:5596.
[43] Zhu XD, Rasing T, Shen YR. Phys Rev Lett 1988;61:2883.
[44] Raschke MB, Höfer U. Phys Rev B 1999;59:2783.
[45] Raschke MB, Höfer U. Phys Rev B 2001;63:201303.
[46] Su X, Lianos L, Shen YR, Somorjai GA. Phys Rev Lett 1998;80:1533.
[47] Denzler DN, Hess C, Dudek R, Wagner S, Frischkorn C, Wolf M, et al. Chem Phys Lett 2003;376:618.

[48] Miranda PB, Xu L, Shen YR, Salmeron M. Phys Rev Lett 1998;81:5876.
[49] Su X, Cremer PS, Shen YR, Somorjai GA. Phys Rev Lett 1996;78:42.
[50] Freund H-J, Ernst N, Risse T, Hamann H, Rupprecher G. Phys Status Solidi 2001;187:257.
[51] Kung KY, Chen P, Wei F, Shen YR, Somorjai GA. Surf Sci 2000;463:L627.
[52] Dellwig T, Rupprechter G, Unterhalt H, Freund H-J. Phys Rev Lett 2000;85:776.
[53] Cremer PS, McIntyre BJ, Salmeron M, Shen YR, Somorjai GA. Catal Lett 1995;34:11.
[54] Volpp HR, Wolfrum J. In: Kohse-Höinghaus K, Jeffries J, editors. Applied combustion diagnostics. Taylor and Francis; 2002.
[55] Su X, Cremer PS, Shen YR, Somorjai GA. J Am Chem Soc 1997;119:3994.
[56] Härle H, Lehnert A, Metka U, Volpp H-R, Willms L, Wolfrum J. Appl Phys B 1999;68:567.
[57] Chin RP, Huang JY, Shen YR, Chuang TJ, Seki H. Phys Rev B 1996;54:8243.
[58] Chin RP, Huang JY, Shen YR, Chuang TJ, Seki H. Phys Rev B 1995;52:5985.
[59] Cremer PS, Su X, Shen YR, Somorjai GA. Catal Lett 1996;40:143.
[60] Cremer PS, Su X, Shen YR, Somorjai GA. J Am Chem Soc 1996;118:2942.
[61] Westerberg S, Wang C, Chen K, Somorjai GA. J Phys Chem B 2004;108:6374.
[62] Harris AL, Levinos NJ. J Chem Phys 1989;90:3878.
[63] Harris AL, Rothberg L, Dubois LH, Levinos NJ, Dahr L. Phys Rev Lett 1990;64:2086.
[64] Sitzmann EV, Eisenthal KB. J Chem Phys 1988;92:4579.
[65] Guyot-Sionnest P. Phys Rev Lett 1991;67:2323.
[66] Ueba H. Prog Surf Sci 1997;55:115.
[67] Guyot-Sionnest P. Phys Rev Lett 1991;66:1489.
[68] Morin M, Jakob P, Levinos NJ, Chabal YJ, Harris AL. J Chem Phys 1992;96:6203.
[69] Bonn M, Hess C, Funk S, Miners JH, Persson BNJ, Wolf M, et al. Science 1999;285:1042.
[70] Bonn M, Hess C, Funk S, Miners JH, Persson BNJ, Wolf M, et al. Phys Rev Lett 2000;84:4653.
[71] Hess C, Wolf M, Roke S, Bonn M. Surf Sci 2002;502–503:304.
[72] Simpson LJ, Furtak TE. J Electroanal Chem 2001;500:163.
[73] Danckwerts M, Savinova E, Pettinger B, Doblhofer K. Appl Phys B 2002;74:653.
[74] Chou KC, Kim J, Baldelli S, Somorjai GA. J Electroanal Chem 2003;554:253.
[75] Tadjeddine A, Rille AL, Pluchery O, Vidal F, Zhang WQ, Peremans A. Phys Status Solidi (a) 1999;175:89.
[76] Baldelli S, Mailhot G, Ross PN, Somorjai GA. J Am Chem Soc 2001;123:7697.
[77] Chou KC, Markovic NM, Kim J, Ross PN, Somorjai GA. J Phys Chem B 2003;107:1840.
[78] Baldelli S, Mailhot G, Ross PN, andd YRS, Somorjai GA. J Phys Chem B 2001;105:654.
[79] Hunt JH, Guyot-Sionnest P, Shen YR. Phys Rev Lett 1987;133:189.
[80] Guyot-Sionnest P, Superfine R, Hunt JH, Shen YR. Chem Phys Lett 1988;144:1.
[81] Du Q, Frezsy E, Shen YR. Science 1994;264:826.
[82] Himmelhaus M, Eisert F, Buck M, Grunze M. J Phys Chem B 2000;104:576.
[83] Saß M, Löbau J, Lettenberger M, Laubereau A. Chem Phys Lett 1999;311:13.
[84] Yang CS-C, Richter LJ, Stephenson JC, Briggman KA. Langmuir 2002;18:7549.
[85] Salafsky JS, Eisenthal KB. J Phys Chem B 2000;104:7752.
[86] Briggman KA, Richter LJ, Stephenson JC. Biophys J 2003;84:4A.
[87] Roke S, Schins J, Muller M, Bonn M. Phys Rev Lett 2003;90:128101.
[88] Zhang D, Shen YR, Somorjai GA. Chem Phys Lett 1997;281:394.
[89] Wei X, Zhunag X, Hong S-C, Goto T, Shen YR. Phys Rev Lett 1999;82:4256.
[90] Kim D, Shen YR. Appl Phys Lett 1999;74:3314.
[91] Chen Z, Shen YR, Somorjai GA. Annu Rev Phys Chem 2002;53:437.
[92] Gracias DH, Zhang D, Lianos L, Ibach W, Shen YR, Somorjai GA. Chem Phys 1999;245:277.
[93] Lahann J, Mitragotri S, Tran TN, Kaido H, Sundaram J, Choi IS, et al. Science 2003;299:371.
[94] Zhang D, Ward RS, Shen YR, Somorjai GA. J Phys Chem B 1997;101:9060.
[95] Kim J, Opdahl A, Chou KC, Somorjai GA. Langmuir 2003;19:9551.
[96] Chen W, Feller MB, Shen YR. Phys Rev Lett 1989;63:2665.
[97] Feller MB, Chen W, Shen YR. Phys Rev A 1991;43:6778.
[98] Opdahl A, Koffas TS, Amitay-Sadovsky E, Kim J, Somorjai GA. J Phys Condens Matter 2004;16:R659.
[99] Wei X, Miranda P, Shen YR. Phys Rev Lett 2001;86:1554.
[100] Heinz TF, Loy MMT, Watson WA. Phys Rev Lett 1985;54:63.
[101] Höfer U, Li L, Ratzlaff GA, Heinz TF. Phys Rev B 1995;52:5264.
[102] Shank CV, Yen R, Hirlimann C. Phys Rev Lett 1983;51:900.
[103] Akhmanov SA, Koroteev NI, Paitian GA, Shumay IL, Galjautdinov MF, Khaibullin IB, et al. Opt Commun 1983;47:202.
[104] Tom HWK, Aumiller GD, Brito-Cruz CH. Phys Rev Lett 1988;60:1438.
[105] Liebsch A. Electronic excitations at metal surfaces. New York: Plenum Press; 1997.
[106] Bennemann KH, editor. Nonlinear optics in metals. Oxford: Clarendon Press; 1998.
[107] Lüpke G. Prog Surf Sci 1999;35:75.
[108] Höfer U. Appl Phys A 1996;63:533.
[109] Suzuki T. Phys Rev B 2000;61:R5117.
[110] Heinz TF, Himpsel HJ, Polange HJ, Burstein E. Phys Rev Lett 1989;63:644.
[111] Daum W, Krause HJ, Reichel U, Ibach H. Phys Rev Lett 1993;71:1234.
[112] McGilp JF. Phys Status Solidi (a) 1999;175:153.
[113] Yeganeh MS, Qi J, Yodh AG, Tamargo MC. Phys Rev Lett 1992;69:3579.
[114] Qi J, Angerer W, Yeganeh MS, Yodh AG, Theis WM. Phys Rev Lett 1995;75:3174.
[115] Pan R-P, Wei HD, Shen YR. Phys Rev B 1989;39:1229.
[116] Hubner W, Benneman KH. Phys Rev B 1989;40:5973.
[117] Reif J, Zink JC, Schneider CM, Kirschner J. Phys Rev Lett 1991;67:2878.
[118] Reif J, Rau C, Matthias E. Phys Rev Lett 1993;71:1931.
[119] Wierenga HA, de Jong W, Prins MWJ, Rasing T, Vollmer R, Kirilyuk A, et al. Phys Rev Lett 1995;74:1462.
[120] Koopmans B, Koerkamp MG, Rasing T, van den Berg H. Phys Rev Lett 1995;74:3692.
[121] Kirilyuk A, Kirilyuk V, Rasing T. J Magn Magn Mater 1999;198:620.
[122] Petukhov AV, Lyubchanskii IL, Rasing T. Phys Rev B 1997;56:2680.
[123] Melnikov AV, Güdde J, Matthias E. Appl Phys B 2002;74:735.
[124] Boyd GT, Shen YR, Hänsch TW. Opt Lett 1986;11:97.
[125] Schaller RD, Saykally RJ, Shen YR, Lagugne-Labarthet F. Opt Lett 2003;28:1296.
[126] Flörsheimer M, Brillert C, Fuchs H. Langmuir 1999;15:5437.
[127] Wang H, Yan ECY, Borguet E, Eisenthal KB. Chem Phys Lett 1996;259:15.

[128] Dadap JI, Shan J, Eisenthal KB, Heinz TF. Phys Rev Lett 1999;83:4045.
[129] Yang N, Angerer WE, Yodh AG. Phys Rev Lett 2001;87:103902.
[130] Neacsu CC, Reider GA, Raschke MB, in review.
[131] Bouhelier A, Beversluis M, Hartschuh A, Novotny L. Phys Rev Lett 2003;90:013903.
[132] Zayats AV, Sandoghdar V. Opt Commun 2000;178:245.
[133] Huang JY, Shen YR. Phys Rev A 1994;49:3973.
[134] Raschke MB, Hayashi M, Lin SH, Shen YR. Chem Phys Lett 2002;359:367.
[135] Chou KC, Westerberg S, Shen YR, Ross PN, Somorjai GA. Phys Rev B 2004;69:153413.
[136] Kemnitz K, Bhattacharyya K, Hicks JM, Pinto GR, Eisenthal KB. Chem Phys Lett 1986;131:285.
[137] Superfine R, Huand JY, Shen YR. Opt Lett 1990;15:1276.
[138] Superfine R, Huand JY, Shen YR. Chem Phys Lett 1990;172:303.
[139] Lamprecht B, Leitner A, Aussenegg FR. Appl Phys B 1999;68:419.
[140] Roke S, Roeterdink WG, Wijnhoven JEGJ, Petukhov AV, Kleyn AW, Bonn M. Phys Rev Lett 2004;91:258302.